

Multi-modal Validation Framework of Mitral Valve Geometry and Functional Computational Models

Sasa Grbic¹, Thomas F. Easley², Tommaso Mansi¹, Charles H. Bloodworth², Eric L. Pierce², Ingmar Voigt¹, Dominik Neumann¹, Julian Krebs¹, David D. Yuh³, Morten O. Jensen², Dorin Comaniciu¹, and Ajit P. Yoganathan²

¹ Imaging and Computer Vision, Siemens Corporate Technology, Princeton, NJ

² The Wallace H. Coulter Department of Biomedical Engineering, Georgia Institute of Technology and Emory University, Atlanta, GA

³ Section of Cardiac Surgery, Department of Surgery, Yale University School of Medicine, New Haven, CT

Abstract. Computational models of the mitral valve (MV) exhibit significant potential for patient-specific surgical planning. Recently, these models have been advanced by incorporating MV tissue structure, non-linear material properties, and more realistic chordae tendineae architecture. Despite advances, only limited ground-truth data exists to validate their ability to accurately simulate MV closure and function. The validation of the underlying models will enhance modeling accuracy and confidence in the simulated results. A necessity towards this aim is to develop an integrated pipeline based on a comprehensive in-vitro flow loop setup including echocardiography techniques (Echo) and micro-computed tomography. Building on [1] we improved the acquisition protocol of the proposed experimental setup for in-vitro Echo imaging, which enables the extraction of more reproducible and accurate geometrical models, using state-of-the art image processing and geometric modeling techniques. Based on the geometrical parameters from the Echo MV models captured during diastole, a bio-mechanical model is derived to estimate MV closure geometry. We illustrate the framework on two data sets and show the improvements obtained from the novel Echo acquisition protocol and improved bio-mechanical model.

1 Introduction

Cardiovascular Disease causes approximately 30% of deaths worldwide among which heart failure is one of the most frequent causes [2, 3]. One of the main contributors to heart failure is mitral valve (MV) disease, especially MV regurgitation (MR) where the MV closure is impaired causing regurgitant back-flow of blood from the left ventricle to the left atrium. Treatment of MR often requires MV replacement or repair surgery to sustain or improve heart function. In recent years, MV repair procedures, where the valve is surgically altered in order to restore its proper hemodynamic function, are being substituted for classical

valve replacements [4–6], showing improved outcomes by demonstrating lower operative mortality, improved long-term survival, and preserved left ventricular function. As the procedures are technically challenging, they require an experienced surgical team to achieve optimal results [5], since the deformation of complex valve anatomy during the intervention, where the heart is stopped, has to be predicted and associated with post-operative implications regarding valve anatomy and function. Having a framework to explore different surgical repair strategies for an individual patient and virtually compute their immediate outcomes would be a desired tool in current clinical practice. It would enable the surgeon to plan the surgical intervention with respect to the direct outcome.

Driven by the widespread prevalence of MV diseases, researchers are developing methods to assess MV anatomy from multiple imaging modalities and simulate its physiology using biomechanical models [7, 8]. However, they do not enable patient-specific personalization of the geometric model, or this process requires tedious manual interactions which limits their clinical applicability.

In recent years, methods have been proposed to personalize the geometric model of the MV using semi-manual or advanced automated algorithms [9]. Using these models, biomechanical computations can be performed based on a personalized patient-specific geometry as in [10]. However, these models rely on a simplified geometrical model, mainly due to the limitations of in-vivo Echo imaging. In order to apply such methods in clinical practice, the first step is to validate the predictive capabilities of simplified models extracted from Echo against ideal models extracted from micro-computed tomography data (μ CT) in a controlled in-vitro environment.

We propose a validation framework for both geometric and biomechanical models extracted from non-invasive modalities. A new controlled experimental setup was developed for MV in-vitro imaging to acquire functional Echo data and high-resolution μ CT images of the MV. Building on [1], we developed a new Echo imaging protocol which significantly improved the image quality. We utilize novel image processing and geometric modeling techniques to extract reproducible geometrical models from both modalities. From the Echo geometrical model during diastole we derive a biomechanical model to estimate MV closure geometry. Compared to the biomechanical model used in [1] we are able to personalize the chordae tree by applying chordae specific rest length parameters. As the in-vitro Echo imaging is similar to routinely acquired transesophageal echocardiogram (TEE) in clinical practice, our framework could be easily transferred to the clinical setting. We illustrate the framework on two in-vitro data sets.

2 In-Vitro Setup

2.1 Mitral Valve Selection and Preparation

Ovine hearts were obtained through a local farmers market and the MVs excised preserving their annular and subvalvular structures. The valve was then

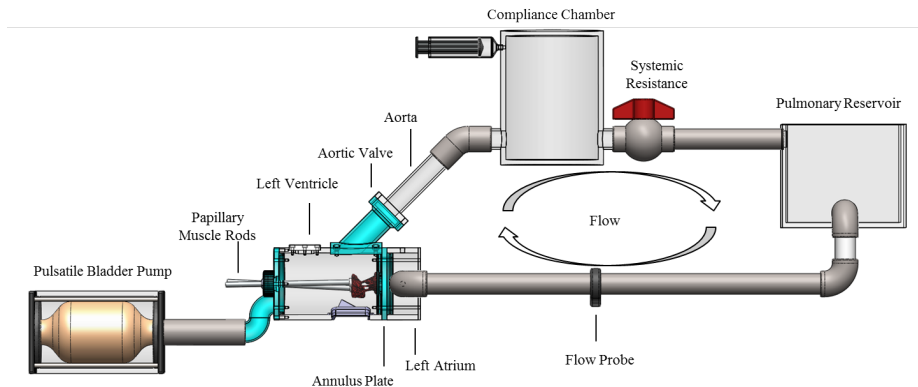


Fig. 1. Schematic of the Georgia Tech Left Heart Simulator (GTLHS) with components identified.

mounted to the annulus plate and mechanical PM positioning system (rods) of the extensively studied Georgia Tech Left Heart Simulator (GTLHS) (Fig. 1) [11, 12].

While suturing the MV to the simulator’s annulus, normal annular-leaflet geometric relationships were respected (anterior leaflet occupying 1/3rd of annular circumference, and commissures in the 2 and 10 o'clock positions).

2.2 Establish Healthy Mitral Valve Geometry and Function In-Vitro

In establishing healthy MV geometry and function, the papillary muscles of the MV were carefully adjusted to positions apically of their respective commissures using previously published techniques [13]. The simulator was tuned to pulsatile human left heart hemodynamics (120 mmHg peak LVP, 5.0 L/min cardiac output, 70 beats/min). Fine adjustments were made to achieve ≈ 6 -8 mm coaptation height at the A2-P2 diameter, minimal leaflet tenting (< 1 mm), and the anterior leaflet consuming 2/3rd of the septal-lateral annular diameter [11]. Upon reaching a healthy control state, the hemodynamics of each valve was recorded over 15 consecutive cardiac cycles. The established healthy control geometry of each valve was held constant over each testing procedure.

2.3 In-Vitro Echocardiography

An novel acoustic window (Fig. 2) was developed for the GTLHS to be used in the new imaging protocol. The acoustic window installed in the posterior of the left ventricle allowed for higher quality acquisition of Rt3DE images compared to the atrial acquisition protocol used in [1]. The window provided a direct echocardiographic view of the chordae and chordal insertions on both the leaflet and the papillary muscles. This view was also closer to the MV leaflets

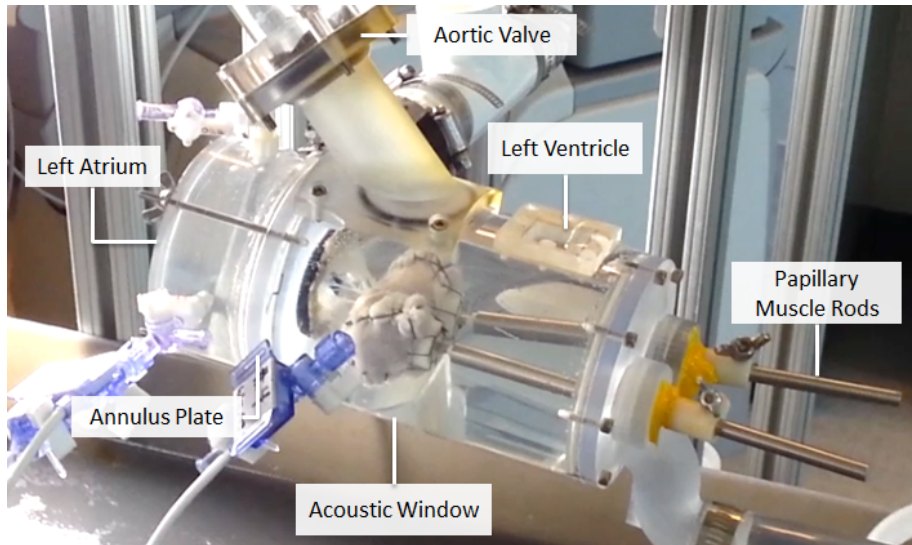


Fig. 2. New left heart chamber for the GTLHS with a smaller size and cylindrical shape for CT scanning, and acoustic window for echocardiography from the left ventricle perspective.

and annulus, allowing the use of a smaller pyramid volume to maximize frame rate. Three-dimensional echocardiography imaging of MVs mounted within the GTLHS was performed using an ie33 Matrix ultrasound system and x7-2 probe (Philips Healthcare; Andover, MA). Zoomed 3D images of the entire mitral complex, including annulus, leaflets, chordae, and papillary muscles were acquired. Acquisition was repeated multiple times from different viewpoints (atrial and ventricular) for optimal image selection. DICOM images were exported for valve segmentation and model generation.

2.4 In-Vitro Micro-computed Tomography

Following echocardiography, the GTLHS was drained of saline and loaded into the new, state-of-the-art Inveon micro-computed tomography scanner (Siemens Medical Solutions USA, Inc.; Malvern, PA). The left heart chamber (LHC) was modified to a smaller size with a cylindrical shape (Fig. 2), which allowed it to fit inside the machine without LHC disassembly. This, in turn, ensured consistent valve geometry (PM positioning) between CT and Rt3DE data sets. The dataset contained the entire mitral valve and was composed of $43.29 \mu\text{m}$ isotropic voxels. The scan was conducted in air with parameters optimized for soft tissue (80 kV energy, $500 \mu\text{A}$ intensity, 500-650 ms integration time). Scans were performed under two MV configurations: open-leaflets (ambient pressure, $\approx 0 \text{ mmHg}$), and closed-leaflets ($\approx 120 \text{ mmHg}$ left ventricular pressure). Acquisitions took under 7 minutes each, leading to minimal tissue dehydration as compared to previ-



Fig. 3. Left: Echo scan of mitral valve (MV) within the in-vitro setting, right: extracted geometric model of the MV. A parachute model of the marginal chordae tendineae are shown in yellow.

ous studies. The μ CT data was exported from the scanners computer and then converted to DICOMs using Siemens Inveon Research Workplace. The DICOMs were then used for computational modeling.

3 Computational Modeling

3.1 Extraction of MV Geometric Model from In-Vitro Echo

We use the anatomical point distribution model of the MV and its subvalvular components from [9, 14] estimated from 3D Echo. The model is hierarchically parametrized containing nine landmarks on the coarse level and two parametric surfaces on the finer scale. The nine landmarks (two trigones, two commissures, one posterior annulus mid-point, two leaflet tips, and two papillary tips) are representing key anatomical landmarks and are capable of capturing a broad spectrum of morphological and physiological variations of the MV physiology. On the finest scale, the model is comprised of the MV annulus, the anterior and posterior leaflets represented as dense surface models.

As the Echo in the in-vitro environment deviates significantly compared to the human TEE scan we adapted our software to manually initialize the geometric model in the in-vitro Echo images. The geometric MV model is further manually refined to match the images. Fig. 3 depicts the extracted model based on the Echo image.

3.2 Biomechanical Model of the Mitral Valve from Echo

We use an extension of the model proposed in [10] to compute the MV closure based on the Echo anatomy. Hereby, the dynamics system $M\ddot{\mathbf{u}} + C\dot{\mathbf{u}} + K\mathbf{u} = \mathbf{f}_t + \mathbf{f}_p + \mathbf{f}_c$ is solved, where M is the diagonal mass matrix calculated from the mass density $\rho = 1040 \text{ g/L}$, C is the Rayleigh damping matrix with coefficients $1e4 \text{ s}^{-1}$ and 0.1 s for the mass and stiffness matrix respectively, K is the

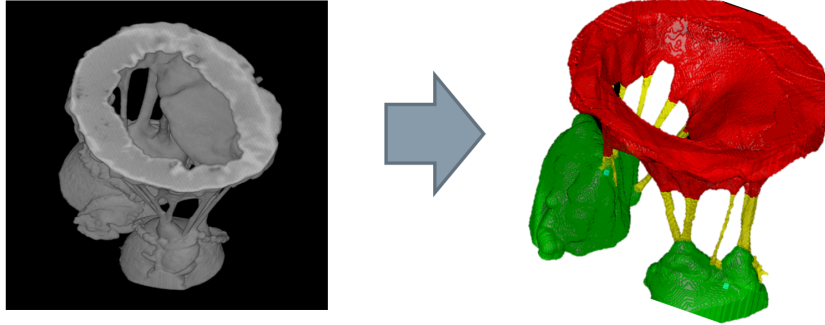


Fig. 4. Left: μ CT scan of mitral valve (MV) within the in-vitro setting, right: extracted geometric model of the MV.

stiffness matrix, \mathbf{f}_t is the force created by the chords on the leaflets, \mathbf{f}_p the pressure force, \mathbf{f}_c the contact forces and \mathbf{u} the displacement. We rely on transverse isotropic linear tissue elasticity, motivated by findings in [15], implemented using a co-rotational finite elements method (FEM) to cope with large deformations. Poisson ratio is set as $\nu = 0.488$ for both leaflets, fiber Young’s modulus is $E_{AL} = 6.23 \text{ MPa}$ and $E_{PL} = 2.09 \text{ MPa}$ for the anterior and posterior leaflets, cross-fiber Young’s modulus is $E_{AL} = 2.35 \text{ MPa}$ and $E_{PL} = 1.88 \text{ MPa}$, and shear modulus is 1.37 MPa . The MV annulus and PMs are fixed. Chordae are modeled as described in [10]: twenty-eight marginal chordae are evenly attached at the free-edges of the leaflets and four chordae are tethered at the base of the leaflets, following an exponential law. The model in [10] was extended to allow personalization of the chordae rest length for each chordae. Self collisions are modeled with collision stiffness of 100 kPa and friction coefficient of 0.1 . We used the SOFA framework⁴ to implement our MV biomechanical model.

Model Personalization Marginal chordae are personalized in a coarse-to-fine approach such that the coaptation line matches accurately. Basal chordae and tissue stiffness are adjusted such that leaflet bowing is captured.

3.3 Extraction of Geometric Model from In-Vitro Micro-computed Tomography

We propose a semi-automated segmentation to extract geometric models of the MV from μ CT images (see Fig. 4), where the final model consists of the MV papillary muscles, chordae tree and MV anterior and posterior leaflets. In the first phase the papillary muscles are segmented by placing manually positive seed points within the anterior and posterior papillary muscles. The Random Walker algorithm [16] is used to delineate the papillary muscle geometry. Next, the MV leaflets are segmented by manually carving the areas of the MV geometric model

⁴ <http://www.sofa-framework.org/>

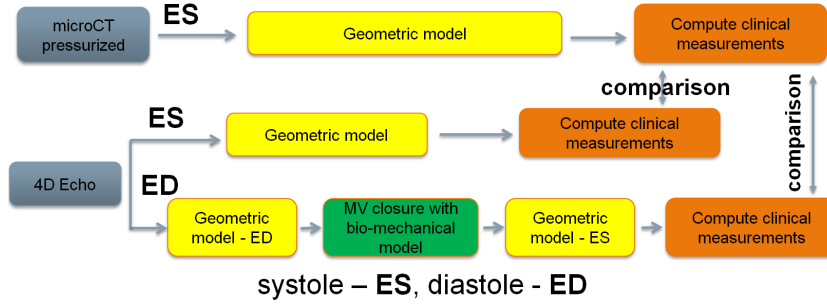


Fig. 5. Validation workflow.

which does not belong to the leaflets. After 4-8 manual iterations the anterior and posterior leaflets are delineated (see red color in Fig. 4). Finally, to extract the final geometric measurements a simplified model (as described in subsection 3.1) is fitted to the extracted model. This model can also be manually refined if necessary.

4 Results

Our framework was utilized on two ovine valves to compare the geometric configuration between the model constructed from Echo and μ CT (considered ground truth) during systole (MV closed). Next, we compute the MV geometry at systole from an end-diastolic (MV open) Echo image and compare it to the ground-truth geometrical configuration obtained from the μ CT image. As the geometric configuration of the MV in the unpressurized μ CT does not correspond with the geometry in Echo during diastole, we only use the closed μ CT image data in our experiments. The reason for this is without a pressure gradient, the suspension in fluid, and flow, the MV leaflets scrunch and become thicker. In addition, the chordae tendineae bunch and it is not possible to delineate the full MV chordae tendineae topology. However, with applied air pressure the leaflet fibers expand to the same geometric configuration as seen in Echo. The complete validation workflow is shown in Fig. 5.

4.1 Geometric Comparison

Based on the geometric models extracted during systole (MV closed) from Echo and μ CT, we measured clinically relevant parameters for short term mitral valve repair (MR) outcome (coaptation length and coaptation area, see Fig. 7, left) in order to quantitatively compare geometric differences between the two models (see Fig. 7, right). Results suggest that the simplified MV geometric model derived from Echo, similar to routinely acquired clinical data, can approximate important clinical measurements for MR within clinically relevant ranges when

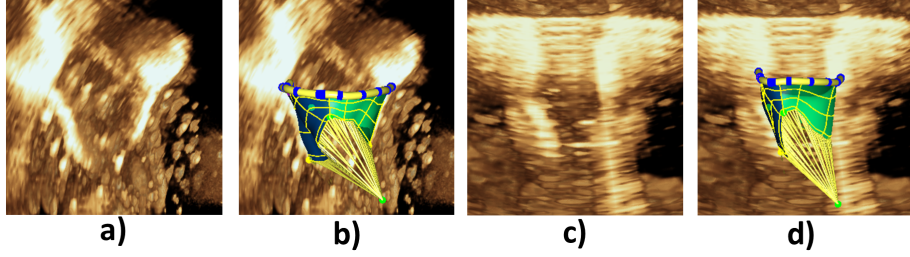


Fig. 6. Comparison of the improved Echo image quality and extracted geometric MV models from the new ventricular imaging protocol (a,b) compared to the atrial protocol used in [1] (c,d).

compared with the idealized geometric model from μ CT. Due to the improved Echo imaging quality (ventricular view) in the new in-vitro setup, we can derive more accurate geometric models of the MV (see Fig. 6 and Fig. 7).

4.2 MV Closure Computation

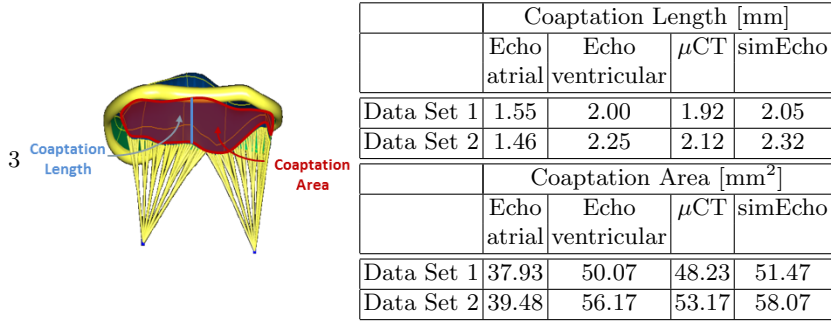


Fig. 7. Geometric comparison of clinical measurements derived from the mitral valve (MV) model at systole from μ CT, old (atrial) Echo acquisition, new (ventricular) Echo acquisition and simulated closure model derived from new (ventricular) Echo acquisition protocol.

We computed MV closure using the biomechanical model (described in Sec. 3.2) starting from the end-diastolic Echo MV model (last frame where the MV is seen open). A generic pressure profile is applied varying from 0 mmHg to 120 mmHg [10] and a time step of 10 ms.

The chord rest length are manually personalized in a coarse-to-fine approach such that the coaptation line matches the Echo data. Finally, to capture the fast dynamics and correctly account for collisions and inertia, pressure increase duration was scaled to last 10 s and 1000 iterations were calculated.

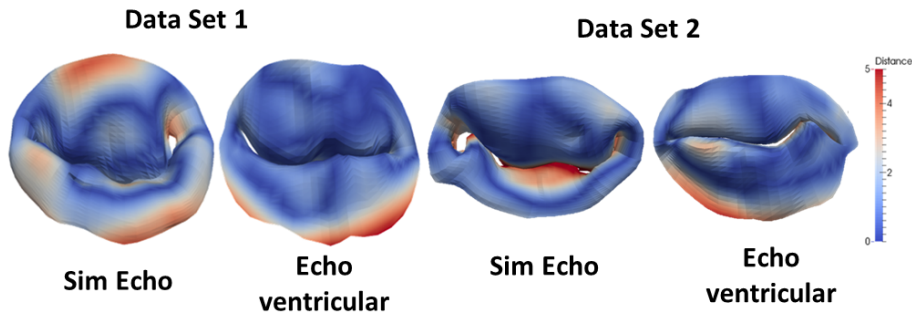


Fig. 8. Qualitative comparison of MV geometry from simulated Echo closure (Sim Echo) and ventricular Echo compared to the ground-truth μ CT model.

Fig. 8 illustrates the geometric distance between the simulated Echo closure (Sim Echo) model, the atrial Echo model, and the ventricular Echo model compared to the ground-truth μ CT model. These results confirm that simplified models from Echo can be utilized to build biomechanical models and compute MV closure geometry in respect to relevant clinical parameters.

5 Conclusion

We extended the framework in [1] for validating geometrical and functional models of the mitral valve (MV) by utilizing a controlled in-vitro setup. We improved the Echo imaging protocol resulting in more accurate and reproducible MV models. In addition, we advanced the bio-mechanical model, allowing for a hierarchical personalization of the marginal and basal chordae rest length parameters. We evaluated our framework by using two ovine data sets. First results are promising, suggesting that the biomechanical model derived from Echo could be accurate enough to model basic clinical biomarkers of MV function. Validation on a larger cohort is under-way.

References

1. Neumann, D., Grbic, S., Mansi, T., Voigt, I., Rabbah, J.P., Siefert, A.W., Saikrishnan, N., Yoganathan, A.P., Yuh, D.D., Ionasec, R.I.: Multi-modal pipeline for comprehensive validation of mitral valve geometry and functional computational models. In: *Statistical Atlases and Computational Models of the Heart. Imaging and Modelling Challenges*. Springer Berlin Heidelberg (2014) 188–195
2. Roger, V.L., Go, A.S., Lloyd-Jones, D.M., Adams, R.J., Berry, J.D., Brown, T.M., Carnethon, M.R., Dai, S., de Simone, G., Ford, E.S., et al.: Heart disease and stroke statistics2011 update a report from the american heart association. *Circulation* **123**(4) (2011) e18–e209
3. Stewart, S., MacIntyre, K., Capewell, S., McMurray, J.: Heart failure and the aging population: an increasing burden in the 21st century? *Heart* **89**(1) (2003) 49–53

4. Vassileva, C.M., Mishkel, G., McNeely, C., Boley, T., Markwell, S., Scaife, S., Hazelrigg, S.: Long-term survival of patients undergoing mitral valve repair and replacement a longitudinal analysis of medicare fee-for-service beneficiaries. *Circulation* **127**(18) (2013) 1870–1876
5. Kilic, A., Shah, A., Conte, J., Baumgartner, W., Yuh, D.: Operative outcomes in mitral valve surgery: Combined effect of surgeon and hospital volume in a population-based analysis. *J. Thorac. Cardiovasc. Surg.* (2012)
6. Borger, M.A., Alam, A., Murphy, P.M., Doenst, T., David, T.E.: Chronic ischemic mitral regurgitation: repair, replace or rethink? *The Annals of thoracic surgery* **81**(3) (2006) 1153–1161
7. Wang, Q., Sun, W.: Finite element modeling of mitral valve dynamic deformation using patient-specific multi-slices computed tomography scans. *Ann. Biomed. Eng.* **41**(1) (2013) 142–153
8. Stevanella, M., Maffessanti, F., Conti, C., Votta, E., Arnoldi, A., Lombardi, M., Parodi, O., Caiani, E., Redaelli, A.: Mitral valve patient-specific finite element modeling from cardiac mri: Application to an annuloplasty procedure. *Cardiovascular Engineering and Technology* **2**(2) (2011) 66–76
9. Ionasec, R., Voigt, I., Georgescu, B., Wang, Y., Houle, H., Vega-Higuera, F., Nassir, N., Comaniciu, D.: Patient-specific modeling and quantification of the aortic and mitral valves from 4-D cardiac CT and tee. *TMI* **29**(9) (2010) 1636–1651
10. Mansi, T., Voigt, I., Georgescu, B., Zheng, X., Assoumou Mengue, E., Hackl, M., Ionasec, Razvan, T., Seeburger, J., Comaniciu, D.: An integrated framework for finite-element modeling of mitral valve biomechanics from medical images: Application to mitralclip intervention planning. *Med. Image Anal.* **16**(7) (2012) 1330–1346
11. Siefert, A.W., Rabbah, J.P.M., Koomalsingh, K.J., Touchton Jr, S.A., Saikrishnan, N., McGarvey, J.R., Gorman, R.C., Gorman III, J.H., Yoganathan, A.P.: In vitro mitral valve simulator mimics systolic valvular function of chronic ischemic mitral regurgitation ovine model. *Ann. Thorac. Surg.* **95** (2013) 825–830
12. Rabbah, J.P., Saikrishnan, N., Yoganathan, A.P.: A novel left heart simulator for the multi-modality characterization of native mitral valve geometry and fluid mechanics. *Ann. Biomed. Eng.* **31** (2012) 305–315
13. Jimenez, J.H., Soerensen, D.D., He, Z., Ritchie, J., Yoganathan, A.P.: Effects of papillary muscle position on chordal force distribution: an in-vitro study. *The Journal of heart valve disease* **14**(3) (2005) 295–302
14. Grbic, S., Ionasec, R., Vitanovski, D., Voigt, I., Wang, Y., Georgescu, B., Comaniciu, D.: Complete valvular heart apparatus model from 4d cardiac ct. *Medical Image Analysis* **16**(5) (2012) 1003–1014
15. Krishnamurthy, G., Itoh, A., Bothe, W., Swanson, J., Kuhl, E., Karlsson, M., Craig Miller, D., Ingels, N.: Stress–strain behavior of mitral valve leaflets in the beating ovine heart. *J. Biomech.* **42**(12) (2009) 1909–1916
16. Grady, L.: Random walks for image segmentation. *IEEE Transactions on Pattern Analysis and Machine Intelligence* **28**(11) (2006) 1768–1783